CD8$^+$ cells regulate the T helper-17 response in an experimental murine model of Sjögren syndrome

X Zhang[1,2], CS Schaumburg[3], TG Coursey[1], KF Siemasko[3], EA Volpe[1], NB Gandhi[1], D-Q Li[1], JY Niederkorn[4], ME Stern[1,3], SC Pflugfelder[1] and CS de Paiva[1]

This study investigated the regulatory function of CD8$^+$ cells in T helper-17 (Th17) cell-mediated corneal epithelial barrier disruption that develops in a murine desiccating stress (DS) model that resembles Sjögren syndrome. CD8$^+$ cell depletion promoted generation of interleukin-17A (IL-17A)-producing CD4$^+$ T cells via activation of dendritic cells in both the ocular surface and draining cervical lymph nodes in C57BL/6 mice subjected to DS. T-cell-deficient nude recipient mice receiving adoptively transferred CD4$^+$ T cells from CD8$^+$ cell-depleted donors exposed to DS displayed increased CD4$^+$ T-cell infiltration and elevated IL-17A and CC-chemokine attractant ligand 20 levels in the ocular surface, which was associated with greater corneal barrier disruption. Enhanced DS-specific corneal barrier disruption in CD8-depleted donor mice correlated with a Th17-mediated expression of matrix metalloproteinases (MMP-3 and MMP-9) in the recipient corneal epithelium. Co-transfer of CD8$^+$CD103$^+$ regulatory T cells did not affect the ability of DS-specific pathogenic CD4$^+$ T cells to infiltrate and cause ocular surface disease in the nude recipients, showing that CD8$^+$ cells regulate the efferent arm of DS-induced immune response. In summary, CD8$^+$ regulatory cells suppress generation of a pathogenic Th17 response that has a pivotal role in DS-induced disruption of corneal barrier function.

INTRODUCTION

Inflammation mediated by CD4$^+$ T cells has a prominent role in many immunologic disorders. T helper-1 (Th1), Th2, and Th17 populations may each be involved in inflammatory processes, reflecting distinct modes of T-cell recruitment, and divergent mechanisms of inflammatory tissue damage.[1,2] Native immune/inflammatory processes are constrained by active cellular quiescence and immunologic tolerance, which offers potential therapeutic approach for enduring control of inflammatory disease. Several regulatory T cells (Tregs) subtypes have been described within each of the two main subcategories, CD4$^+$ Treg and CD8$^+$ Treg.[3,4] Several subsets of inhibitory CD8$^+$ Treg have been identified, some of which may have immunotherapeutic values. Evidence has accumulated that specialized CD8$^+$ Treg have the potential to suppress host injurious responses that develop in autoimmune disorders, such as rheumatoid arthritis, systemic lupus erythematosus, and multiple sclerosis.[4–7]

The Th17 lineage has been found be distinct from traditional Th1 and Th2 lineages. Interleukin-17A (IL-17A)-producing Th17 cells have been identified as a key effector in a variety of human and experimental autoimmune diseases, including Sjögren syndrome (SS), multiple sclerosis, rheumatoid arthritis, systemic lupus erythematosus, and psoriasis.[8,9]

Keratoconjunctivitis sicca (KCS) in SS is a severe and potentially sight-threatening ocular surface epithelial disease. The pathogenesis of KCS in our mouse model of SS is a multifactorial process that includes activation of stress pathways in the ocular surface epithelia by the hyperosmolar tear film and cytokines produced by resident intraepithelial lymphocytes and infiltrating Th1 and Th17 cells.[10–13] In this model, we previously demonstrated that desiccating stress (DS)-activated CD4$^+$ T cells when adoptively transferred to naive T-cell-deficient nude mice, were sufficient to elicit autoimmune lacrimal KCS with features resembling human SS, suggesting that CD4$^+$ T cells make a prominent contribution

[1]Ocular Surface Center, Cullen Eye Institute, and the Department of Ophthalmology, Baylor College of Medicine, Houston, Texas, USA. [2]Department of Ophthalmology, Shenyang He Eye Hospital, Shenyang, Liaoning Province, China. [3]Department of Biological Sciences, Allergan, Irvine, California, USA and [4]Department of Ophthalmology, University of Texas Southwestern Medical Center, Dallas, Texas, USA. Correspondence: CS de Paiva, (cintiadp@bcm.tmc.edu)

Received 14 May 2013; revised 23 July 2013; accepted 3 August 2013; published online 11 September 2013. doi:10.1038/mi.2013.61

to mucosal and glandular inflammation and tissue damage in SS.[14] We have previously demonstrated a suppressive function of $CD4^+CD25^+$ $Foxp3^+$ Treg in $CD4^+$ T-cell-mediated KCS using this model;[14] however, the contribution of $CD8^+$ Treg in this DS model has not been investigated. $CD8^+$ cells have been found to reside in the epithelium and stroma of normal human and mouse conjunctiva, and a significant decrease in $CD8^+$ cells with concomitant increase in CD4/CD8 ratio in the conjunctiva has been observed in human KCS and in our experimental KCS model.[15–18]

Herein, we show for the first time that a subset of $CD8^+$ Tregs can significantly mitigate Th17-mediated disease in our SS model. $CD8^+$ cell depletion augmented pathogenic Th17 cell generation, and consequently worsened IL-17A-induced disruption of corneal barrier function.

RESULTS

The effect of DS on $CD8^+$ population

We have previously observed a significant decrease in $CD8^+$ cells with a concomitant increase in CD4/CD8 ratio in the conjunctiva in our DS model of SS.[15] A significant increase in the number of $CD8^+$ lymphocytes was noted in the draining cervical lymph nodes (CLNs) after DS by flow cytometry (**Figure 1a**).

$CD8^+CD122^+$ and $CD8^+CD103^+$ T cells are recently identified Treg populations that can suppress $CD4^+$ T-cell proliferation.[19–23] Rare $CD8^+CD122^+$ Tregs were noted in the ocular surface and CLN, and no obvious change was found in the number of $CD8^+CD122^+$ cells in CLN after DS by flow cytometry analysis (**Figures 1b and c**). By contrast, $61.3 \pm 3.8\%$ of $CD8^+$ lymphocytes in CLN were noted to co-express CD103, and the number of these $CD8^+CD103^+$ cells significantly increased after DS (**Figures 1d–g**).

The number of $CD8^+CD103^+$ cells also increased on the ocular surface after DS (**Figures 1e–g**). We have previously surveyed the conjunctiva regarding the presence of intra-epithelial lymphocytes[24] and we have found that there is no increase in the percentage of total $CD3^+$ cells during DS.[24] This evidence suggests that $CD8^+CD103^+$ cells may be one of the cell populations regulating the autoimmune inflammation that develops in this model.

$CD8^+$ cell depletion promoted activation of ocular surface DCs during DS

Antigen-captured dendritic cells (DCs) at the ocular surface migrate to the CLN to present antigens to T cells. To evaluate the effect of $CD8^+$ cell depletion on DC activation, we performed flow cytometry analysis of freshly isolated cells from the ocular surface and CLN in mice with and without $CD8^+$ cell depletion during DS. We found a significant or progressive decrease in the number of $CD11c^+$ and $CD11b^+$ cells in the ocular surface, accompanied by a progressive increase in the number of these cells in the CLN after exposure to DS. Dual label of these cells with antibody to the murine human leukocyte antigen-class 2 antigen, IAIE, showed that there was a parallel change in DC activation (**Figure 2a**), indicating that DS promoted activation and migration of DCs from the ocular surface.

Both local and systemic $CD8^+$ cell depletion increased the number and activation of DCs in the ocular surface, while they had no effect in the number and activation of DCs in the draining CLN after DS1 (**Figure 2a**). Immunohistochemical staining of $CD11c^+$ cells in the conjunctiva confirmed the flow cytometry results, showing a significantly increased number of $CD11c^+$ cells in the $CD8^+$ cell-depleted group compared with the isotype control group after 1 day of DS (DS1; **Figures 2b and c**). These findings indicate that $CD8^+$ cell depletion promoted the accumulation and activation of DCs in the ocular surface after DS1. After DS5, the number of activated DCs decreased in the ocular surface and increased in the draining CLN (**Figure 2a**), indicating that $CD8^+$ cell depletion promoted the migration of DCs from the ocular surface to the regional node at this stage.

$CD8^+$ cell depletion promoted Th17 cell generation during DS

In our murine model of SS, we previously demonstrated that DS generated Th1 and Th17 cells pathogenic $CD4^+$ T cells that are capable of adoptively transferring dry eye disease to T-cell-deficient nude mice.[11,12,14,25] Immunohistochemical staining of $CD4^+$ cells in the ocular surface showed that the number of $CD4^+$ cells in the conjunctiva significantly increased in the systemic CD8-depleted group compared with the isotype control group after DS5 (**Figure 2e**). No $CD4^+$ T-cell infiltration was found in the cornea of non-stressed (NS), DS5 and the isotype antibody-treated controls; however, $CD4^+$ T-cell infiltration was noted in the corneas of DS5 mice systemically treated with the anti-CD8 antibody (**Figure 2e**). We found that systemic $CD8^+$ cell depletion significantly increased the number of $CD4^+$ T cells in the draining CLN after DS5, as determined by flow cytometry (**Figure 2f**). Local depletion of $CD8^+$ cells yielded a similar increase in the number of $CD4^+$ T cells in the ocular surface and draining CLN as systemic $CD8^+$ cell depletion (data not shown). Using absolute cell counts (total splenocytes) normalized by the number of spleens, we observed that there was no difference in the total number of starting cells among all groups (NS: 8.95 ± 2.04; DS5: 7.47 ± 1.50; isotype control: 7.53 ± 1.66 and systemic anti-CD8: $8.27 \pm 1.52 \times 10^7$ total cells) but the recovery of $CD4^+$ cells was higher in the CD8-depleted group (NS: 6.08 ± 2.17; DS5: 5.60 ± 0.83; isotype control: 6.07 ± 2.04 and systemic anti-CD8: $10.22 \pm 3.8 \times 10^6$ isolated $CD4^+$ T cells, $P = 0.03$ between IC treated and systemic CD8 treated). Taking together, these findings suggest that CD8 neutralization enhanced the generation of autoreactive $CD4^+$ T cells following DS.

The absence of obvious differences in DC activation and $CD4^+$ T-cell generation between the local (subconjunctival injection) and systemic $CD8^+$ cell antibody depletion groups prompted evaluation of the efficiency of $CD8^+$ cell depletion. Flow cytometric analysis of freshly isolated CLN cells from CD8 or isotype antibody-treated mice showed that both local and

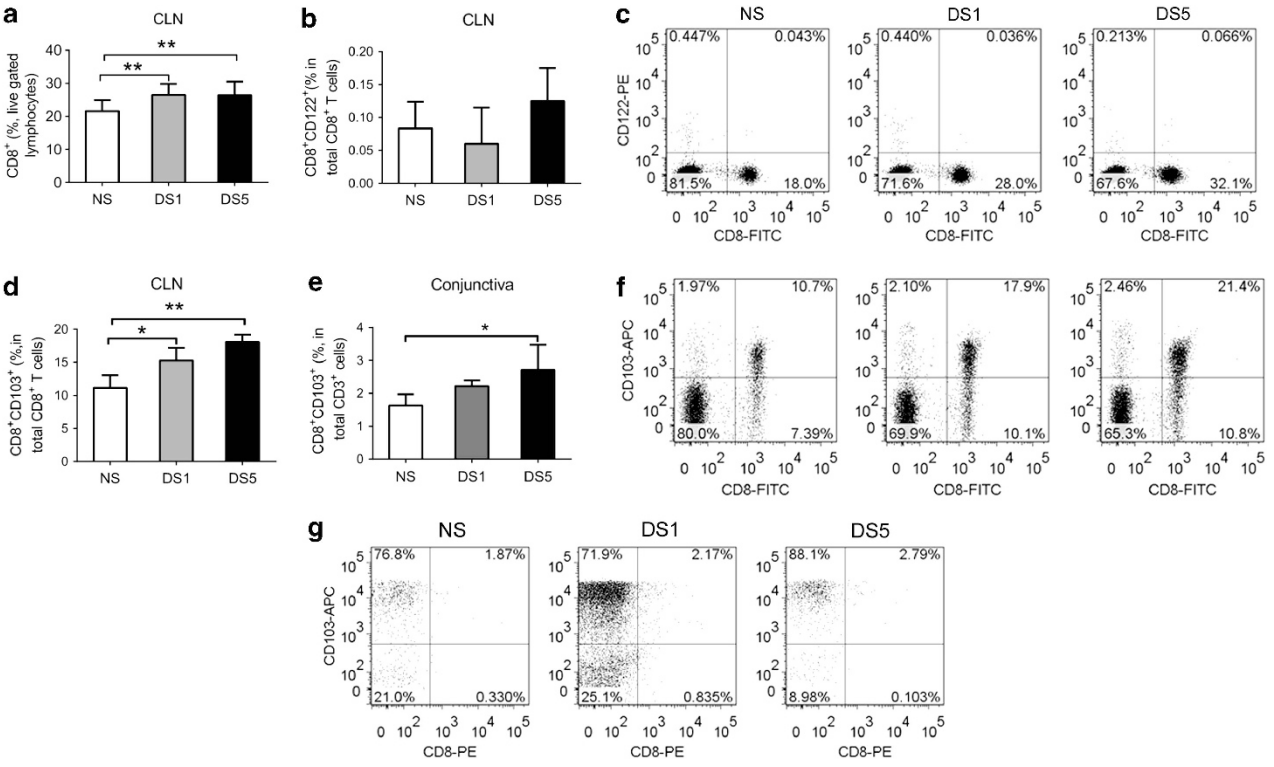

Figure 1 The effects of desiccating stress (DS) on CD8$^+$ cell population. (**a**) Mean ± s.d. of flow cytometry analysis of CD8$^+$ lymphocytes in draining cervical lymph nodes (CLN) in non-stressed (NS) controls and after DS for 1 (DS1) or 5 (DS5) days. Experiments were performed two times with at least four mice per group per experiment; **Indicates $P<0.01$ comparison. (**b**) Mean ± s.d. of flow cytometry analysis of CD8$^+$CD122$^+$ lymphocytes in draining CLN in NS, DS1, and DS5 groups. Experiments performed two times with at least four mice per group per experiment. (**c**) Representative dot plots of an experiment showing cells isolated from CLN dual stained for CD8 and CD122. Lymphocytes were gated based on characteristic light-scatter properties, single lymphocytes were gated based on forward scatter height vs. forward scatter area (FSC-A) and live–dead exclusion by propidium iodide. Numbers in the quadrants indicate the percentage of cells. (**d**) Mean ± s.d. of flow cytometry analysis of CD8α$^+$CD103$^+$ lymphocytes in draining CLN in NS, DS1 and DS5 groups. Experiments were performed two times with at least four mice per group per experiment. *Indicates $P<0.05$ comparison; **indicates $P<0.01$ comparison. (**e**) Mean ± s.d. of flow cytometry analysis of CD8α$^+$ CD103$^+$ T cells in the ocular surface of NS, DS1, and DS5 groups. Experiments were performed two times with two to three mice per group per experiment. (**f**) Representative dot plots of an experiment showing cells isolated from CLN dual stained for CD8 and CD103 in NS, DS1, and DS5 groups. Lymphocytes were gated based on characteristic light-scatter properties, single lymphocytes were gated based on forward scatter height vs. FSC-A and live–dead exclusion by propidium iodide. Numbers in the quadrants indicate the percentage of cells. (**g**) Representative dot plots of an experiment showing cells isolated from the conjunctiva and stained for CD3, CD8, and CD103. Lymphocytes were gated based on characteristic light-scatter properties, single lymphocytes were gated based on forward scatter height vs. FSC-A and live–dead cell discrimination was obtained by propidium iodide staining. CD8 and CD103-positive cells were gated from CD3-positive cells. Numbers in the quadrants indicate the percentage of cells. Experiments were repeated two times with two to three mice per group per experiment.

systemic injection of anti-CD8 effectively depleted CD8α$^+$ (isotype control: 23.13 ± 6.23%; local anti-CD8: 0.70 ± 0.26%; systemic anti-CD8: 0.82 ± 0.29%) and CD8β$^+$ cells (isotype control: 26.97 ± 4.06%; local anti-CD8: 1.1 ± 0.14%; systemic anti-CD8: 0.92 ± 0.33%). No significant difference was found in the efficiency of CD8$^+$ cell depletion between the local and systemic antibody-treated groups ($P>0.05$), suggesting that in addition to local effect, subconjunctival injected anti-CD8 antibody drained to CLN and produced an effect similar to systemically injected antibody.

We found increased production of IL-17A in both ocular surface cells and CD4$^+$ T cells, whereas decreased production of interferon-γ (IFN-γ) was noted in the ocular surface cells and decreased expression of IL-13 was noted in the CD4$^+$ T-cell population by ELISPOT (**Figure 3a**) in the CD8-depleted group when compared to IC treated group. Furthermore, real-time PCR performed on isolated CD4$^+$ T cells confirmed expression of the Th signature cytokines and their respective transcription factors (Th17: IL-17A and RORγT; Th1: IFN-γ and T-bet; Th2 cytokine, IL-13 and GATA-3) that was observed by ELISPOT in mice after DS5 with and without systemic CD8$^+$ cell depletion (**Figure 3b**). These findings suggest that CD8$^+$ cell depletion exerted the most prominent effect on the generation of pathogenic Th17 cells during DS.

CD8$^+$ cell depletion worsened pathogenic Th17-mediated corneal barrier disruption

To investigate the effects of CD8$^+$ cell depletion on generation of pathogenic Th17 cells, we compared corneal and conjunctiva disease severity following CD4$^+$ T-cell adoptive transfer into T-cell-deficient nude recipient mice. We found that adoptive transfer of CD4$^+$ T cells from CD8$^+$ cell-depleted DS5 donor mice increased CD4$^+$ T-cell infiltration in the recipient conjunctiva compared with the isotype control group

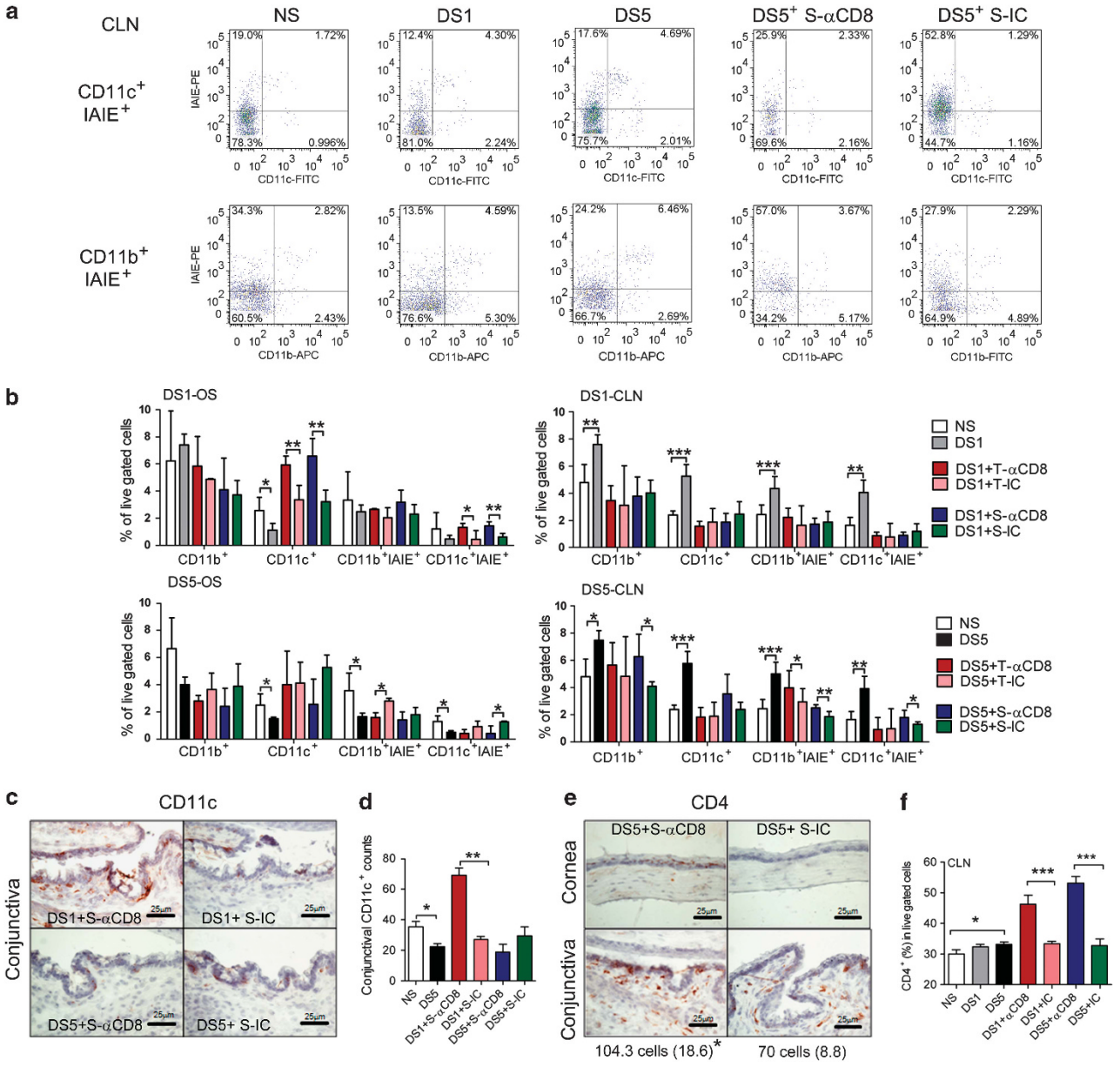

Figure 2 The effects of CD8$^+$ cell depletion on dendritic cell (DC) activation. (**a**) Representative flow cytometry dot plot analysis of dual CD11c$^+$IAIE$^+$ and dual CD11b$^+$IAIE$^+$ cells in the draining cervical lymph node (CLN) in non-stressed (NS) controls and after desiccating stress (DS) for 1 (DS1) or 5 (DS5) days and mice that received systemic (S) injection of anti-CD8 (αCD8) antibody or isotype control (IC) antibody after DS5 treatment. CD11c and CD11b cells were gated based on characteristic light-scatter properties, single cells were gated based on forward scatter height vs. forward scatter area and live–dead cell discrimination was obtained by propidium iodide staining. Numbers in the quadrants indicate the percentage of cells. Experiments were performed two times with at least four mice per group per experiment. (**b**) Mean ± s.d. of flow cytometry analysis of single-cell suspensions isolated from the ocular surface (OS) or CLN stained for CD11c$^+$, CD11b$^+$ or dual stained with the major histocompatibility complex (MHC) II marker, IAIE in NS, DS1, DS5 and mice that received either S or topical (T) injections of anti-CD8 (αCD8) antibody or IC antibody after DS1 or DS5 treatment. Experiments were performed two times with at least four mice per group per experiment. *$P<0.05$; **$P<0.01$, ***$P<0.001$. (**c**) Representative images of immunohistochemical CD11c$^+$ staining in the conjunctiva of C57BL/6 mice that received S injection of anti-CD8 (αCD8) antibody or IC antibody after DS1 or DS5 treatment. (**d**) Bar graph showing mean ± s.d. the number of CD11c$^+$ cells in the conjunctiva of C57BL/6 mice that received S injection of anti-CD8 (αCD8) antibody or IC antibody after DS1 or DS5 treatment. *$P<0.05$; **$P<0.01$. Experiments were performed two times with at least two to three mice per group per experiment. (**e**) Representative images of immunohistochemical CD4$^+$ staining in the cornea and conjunctiva of C57BL/6 mice that received systemic injection of αCD8 antibody or IC antibody after DS1or DS5 treatment. (**f**) Mean ± s.d. of flow cytometry analysis of CD4$^+$ cells in draining cervical lymph nodes in NS, DS1, DS5, and DS1/5 mice that received either systemic injection of anti-CD8 (αCD8) antibody or IC antibody. Lymphocytes were gated based on characteristic light-scatter properties, single cells were gated based on forward scatter height vs. forward scatter area and live–dead cell discrimination was obtained by propidium iodide staining. Experiments were performed two times with at least four mice per group per experiment. *$P<0.05$; ***$P<0.001$.

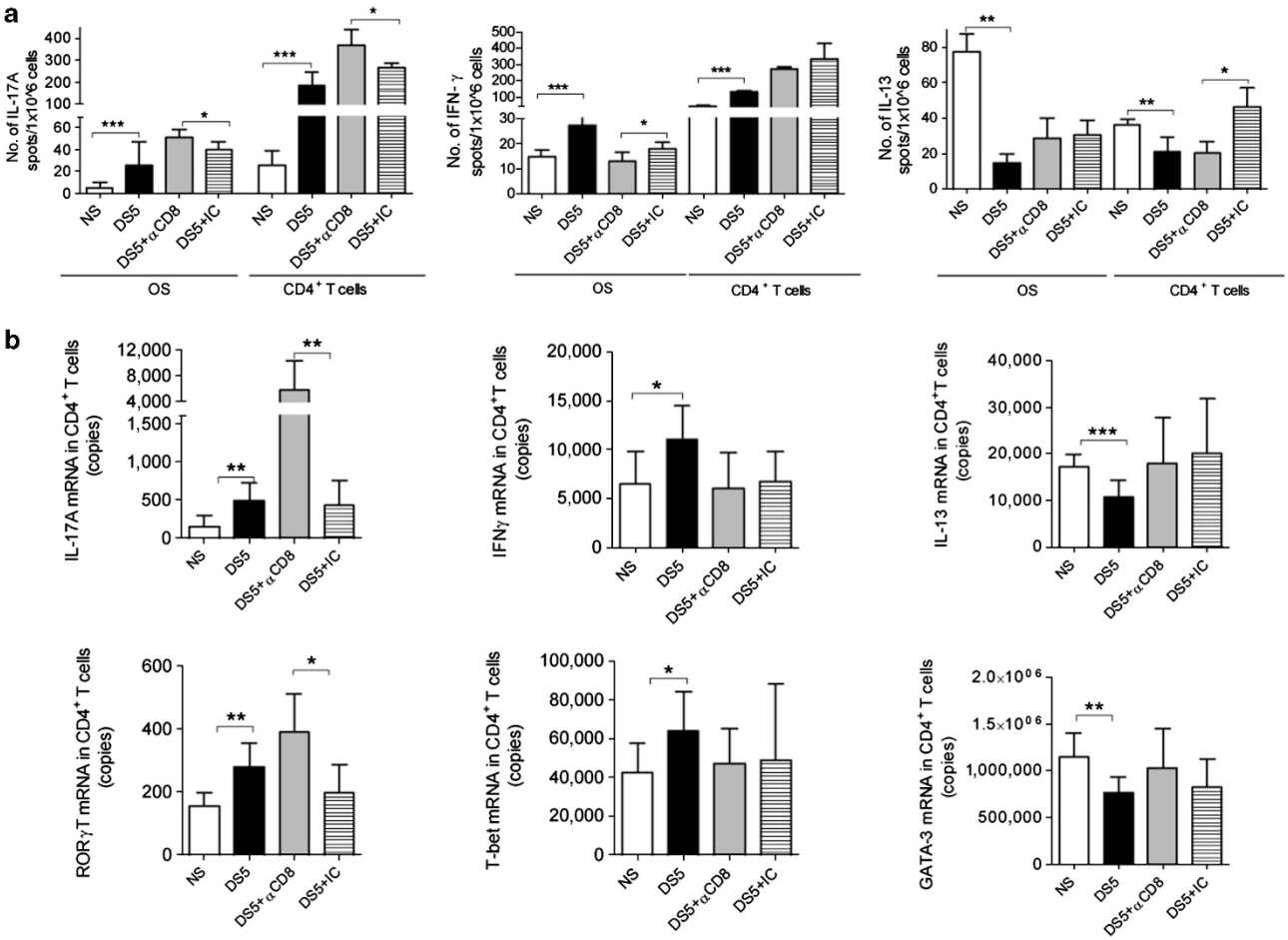

Figure 3 The effects of CD8$^+$ cell depletion on CD4$^+$ T population. (**a**) Results of ELISPOTs to detect interleukin-17A (IL-17A), interferon-γ (IFN-γ), and IL-13-producing cells isolated from the ocular surface (OS) and CD4$^+$ T cells isolated from spleen and cervical lymph nodes (CLNs) of C57BL/6 before (non-stressed, NS) or after DS5 in mice that received systemic injection of αCD8 antibody or isotype control (IC) antibody after desiccating stress for 5 (DS5) treatment. Experiments were performed two times with five mice per group per experiment. (**b**) Gene expression analysis showing copies of IL-17A, IFN-γ, IL-13, RORγT, T-bet, and GATA-3 transcripts in the CD4$^+$ T cells isolated from spleen and cervical lymph node (CLN) of C57BL/6 before (NS) or after DS5 in mice that received systemic injection of αCD8 antibody or IC. *$P<0.05$; **$P<0.01$; ***$P<0.001$. Experiments were performed three times with three to four mice per group per experiment.

(**Figures 4a and b**). Reduced CD4$^+$ T-cell infiltration was noted in corneas of the recipients receiving CD4$^+$ T cells from isotype control antibody-treated DS5 donor mice (2/5 mice); however, widespread CD4$^+$ T infiltration was noted in corneas of all recipients of CD4$^+$ T cells from DS5 donor mice with CD8$^+$ cell depletion (5/5 mice; **Figure 4b**).

To further confirm the role of CD8$^+$ cell depletion on generation of Th17 cells, we evaluated IL-17A and CC-chemokine attractant ligand 20 (CCL20) gene expression in the recipient corneal epithelia and conjunctiva as Th17 committed cells produce IL-17A and CCL20, among other mediators.[26,27] Our results show that CD8$^+$ cell depletion significantly increased levels of IL-17A (cornea and conjunctiva) and CCL20 mRNA transcripts (cornea; **Figures 4c–f**).

We have previously shown that IL-17A has a pathogenic role in the corneal disease that develops in an experimental murine model of SS.[13] To confirm the effect of CD8$^+$ cell depletion on generation of Th17 cells capable of causing corneal epithelia disease, we evaluated corneal barrier function in the CD4$^+$ adoptive transfer recipients. As seen in **Figures 4g and h**, mice that received CD4$^+$ T cells from CD8-deficient mice showed greater corneal barrier disruption function than recipients of isotype control-treated mice.

To determine if CD8$^+$ cell depletion augments the IL-17A-mediated matrix metalloproteinase (MMP) production, we evaluated expression of MMP-3 and MMP-9 in the corneal epithelia of adoptive transfer recipients. We found significantly increased immunoreactivity to MMP-3 and MMP-9 in the recipients of CD4$^+$ T cells from CD8$^+$ cell-depleted donors (**Figures 4i–k**). Both *in situ* zymography in corneal cryosections and real-time PCR further confirmed the results of immunostaining as there was increased gelatinase activity and increased expression of MMP-3 and MMP-9 mRNA transcripts in the corneal epithelia of the CD8$^+$ cell-depleted recipient group compared with recipients of the isotype control-treated group (**Figures 4i–n**).

Co-transfer of CD8$^+$CD103$^+$ Treg did not suppressed the Th17 pathogenic response in the ocular surface

The integrin CD103 (α_E/β_7) is widely expressed on intraepithelial CD8$^+$ T cells.[28] In the conjunctiva, we also found CD8$^+$ cells co-express CD103 (**Figure 1**). To investigate the role of CD8$^+$CD103$^+$ Treg in regulating migration of pathogenic Th17 cells generated in mice exposed to DS, CD8$^+$CD103$^+$ Tregs were co-adoptively transferred with

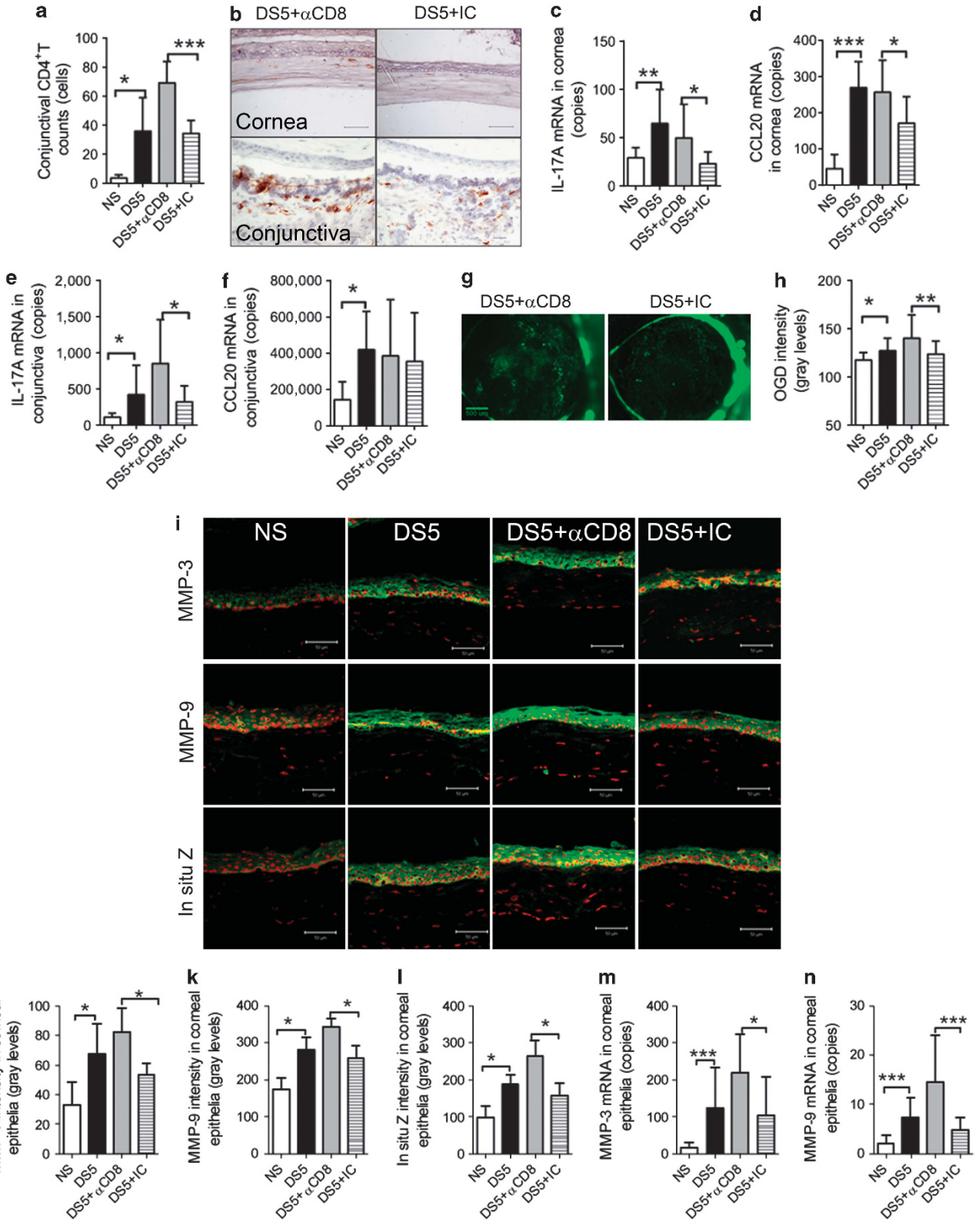

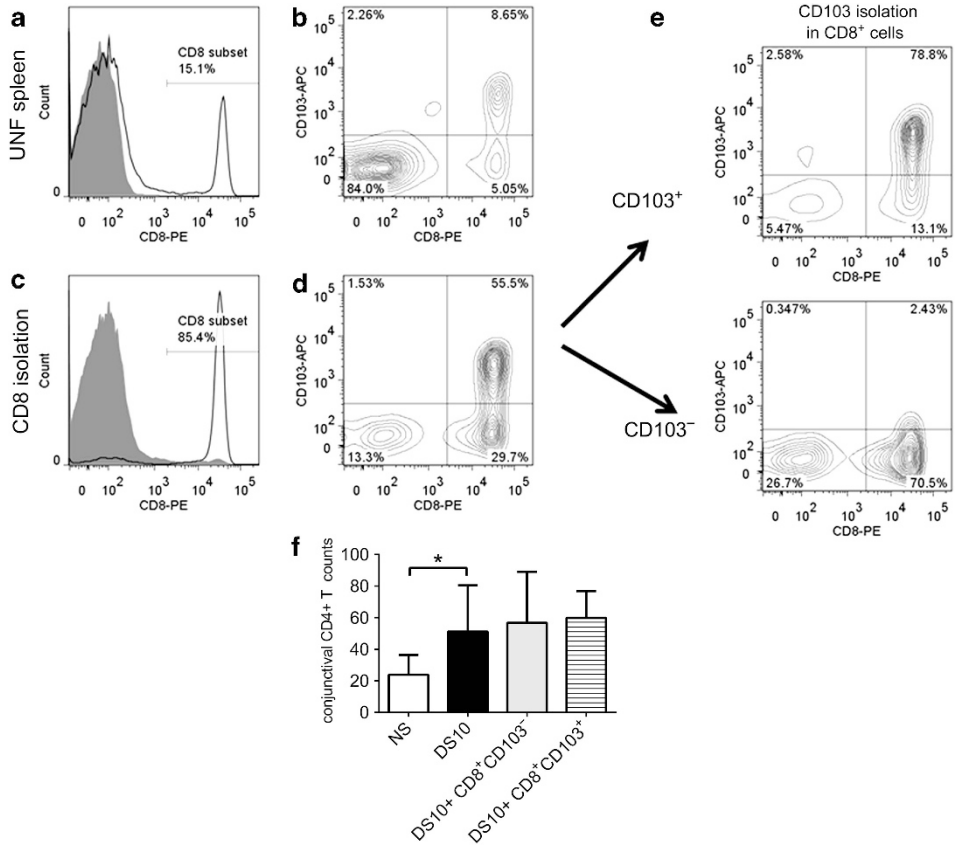

Figure 5 $CD8^+CD103^+$ isolation using magnetic beads and co-adoptive transfer results. (**a**) Unfractionated (UNF) splenocytes were stained for CD8 (white histogram) and showed ~15% $CD8^+$ T cells (isotype control antibody, shaded histogram). (**b**) About 50% of $CD8\alpha^+$ T cells are also $CD103^+$. (**c**) Histogram showing successful separation of $CD8^+$ (white histogram) and CD8 negative cells (shaded histogram). (**d**) In all, 55.5% of isolated $CD8^+$ cells co-express CD103 marker. (**e**) $CD8^+$ T cells were further isolated based on the expression of CD103: $CD103^+$ expression increased to 78.8% in the positive population, whereas the negative population had just 2.43% of double positive cells. (**f**) Bar graph showing the number of $CD4^+$ T cells in the conjunctiva of nude mouse adoptive transfer recipients of $CD4^+$ T cells. Nude mouse recipients were divided into four groups in this experiment: (1) non-stressed (NS) that received $CD4^+$ T cells from NS B6 mice; (2) DS10 that received $CD4^+$ T cells from DS10 B6 mice; (3) DS10 + $CD8^+CD103^+$ Treg mice that received $CD4^+$ T cells from DS10 B6 mice and $CD8^+CD103^+$ (2×10^6); and (4) DS10 + $CD8^+CD103^-$ mice that received $CD4^+$ T cells from DS10 B6 mice and $CD8^+CD103^-$ (2×10^6). Experiments were performed twice with at least two to three mice per group per experiment. $^*P < 0.05$.

Figure 4 The effects of pathogenic T helper-17 (Th17) cells stimulated by $CD8^+$ cell depletion on corneal disease. (**a**) Bar graph showing the number of $CD4^+$ T cells in the conjunctiva of nude mouse adoptive transfer recipients of $CD4^+$ T cells from non-stressed (NS) controls, desiccating stress for 5 (DS5) donor days or DS5 donor mice subjected to systemic injection of anti-CD8 (αCD8) antibody or isotype control (IC) antibody. Experiments were performed two times with at least two to three mice per group per experiment. (**b**) Representative images of $CD4^+$ immunohistochemical staining in the cornea and conjunctiva (CJ) of T-cell-deficient (nude) recipient mice following adoptive transfer of $CD4^+$ T cells from DS5 donor mice who received anti-CD8 or isotype antibody after DS5 treatment. (**c**, **d**) Gene expression analysis showing copies of interleukin-17A (IL-17A) (**c**) and CC-chemokine attractant ligand 20 (CCL20) mRNA (**d**) transcripts in recipient corneal epithelia. Experiments were performed three times with three to four mice per group per experiment. (**e**, **f**) Gene expression analysis showing copies of IL-17A (**e**) and CCL20 mRNA (**f**) transcripts in recipient conjunctiva. Experiments were performed three times with three to four mice per group per experiment. (**g**) Representative images of Oregon-green-dextran (OGD) corneal staining in the adoptive transfer recipients of $CD4^+$ T cells obtained from DS5 donor mice, which received anti-CD8 or isotype antibody. Experiments were performed three times with five mice per group per experiment (total of 30 eyes per group). (**h**) Mean ± s.d. of OGD staining intensity in corneas of nude mouse adoptive transfer recipients. Experiments were performed three times with at least five mice per group per experiment. (**i**) Laser scanning immunofluorescent confocal microscopy of cornea stained for matrix metalloproteinases (MMP)-3 and MMP-9 and *in situ* zymography (*in situ* Z) in the adoptive transfer recipients of $CD4^+$ T cells isolated from donor mice who received systemic injection of anti-CD8 (αCD8) or isotype control (IC) antibody during 5 days of desiccating stress (DS5). Experiments were performed two times with two to three mice per group per experiment. (**j–l**) Bar graphs showing mean ± s.d. of fluorescence intensity measured in the corneal epithelium of adoptive transfer recipients for MMP-3 (**j**), MMP-9 (**k**), and *in situ* Z (**l**). Experiments were performed two times with two to three mice per group per experiment. (**m**, **n**) Gene expression analysis showing copies of MMP-3 (**m**) and MMP-9 (**n**) mRNA transcripts in cornea epithelia of adoptive transfer recipients. Experiments were performed two times with two to three mice per group per experiment. NS, nude mice that received $CD4^+$ T cells from NS donor mice; DS5, nude mice that received $CD4^+$ T cells from 5 days of DS donor mice; DS5 + αCD8 and DS5 + IC, nude mice that received $CD4^+$ T cells from DS5 donor mice that received systemic injection anti-CD8 (αCD8) antibody or IC antibody $^*P < 0.05$; $^{**}P < 0.01$; $^{***}P < 0.001$.

$CD4^+$ T cells from mice subjected to DS10 to nude recipients. Efficiency of isolation was confirmed by flow cytometry (**Figures 5a–e**). We found that intraperitoneally (i.p.) injected $CD8^+CD103^+$ Tregs homed to the conjunctiva (data not shown) but did not regulate the number of $CD4^+$ T cells infiltrating the ocular surface (**Figure 5f**) nor conjunctival goblet cell density (data not shown). These findings suggest that $CD8^+CD103^+$ Treg can suppress the generation of pathogenic Th17 cells of this murine SS model before priming by suppressing DC activation but not by blocking the efferent arm of the immune response.

DISCUSSION

This study demonstrated the suppressive effects of $CD8^+$ Treg on Th17 cell-mediated corneal epithelial barrier disruption in our DS model resembling SS. A compensatory increase in $CD8^+$ cells consisting primarily of $CD8^+CD103^+$ Tregs was noted in the draining nodes over the 5-day exposure to DS. $CD8^+$ cell depletion promoted the generation of IL-17A-producing $CD4^+$ T cells via activation of DCs in mice subjected to DS. T-cell-deficient nude recipient mice receiving adoptive transfer of $CD4^+$ T cells from $CD8^+$ cell-depleted donors exposed to DS displayed increased $CD4^+$ T-cell infiltration and enhanced DS-specific Th17-mediated corneal barrier disruption. Co-transfer of $CD8^+CD103^+$ regulatory T cells had no effect on the ability of DS-specific pathogenic $CD4^+$ T cells to infiltrate and cause ocular surface disease in the nude recipients.

A progressive increase in $CD8^+$ lymphocytes was noted in the draining CLNs in mice subjected to DS. Our findings suggest that these $CD8^+$ cells function to regulate the initiation of the autoimmune keratoconjunctivitis that develops in this model. In fact, a compensatory Treg response has been noted during the progression of disease in other autoimmune models. For instance, $CD4^+$ Tregs accumulate to a higher frequency within the CNS of mice with experimental autoimmune encephalomyelitis.[29] Therefore, based on this finding, we hypothesized that the increase in CD8 cells in the CLN is an immunoregulatory response to the DS-induced ocular surface autoimmunity.

In this study, we found that depletion of $CD8^+$ regulatory cells stimulated DC activation and homing during immunopathogenesis of this DS-induced SS model. Systemic $CD8^+$ cell depletion promoted resident ocular surface DC recruitment and activation at an early stage (day 1) of DS treatment, while it enhanced migration of ocular surface DCs at a late stage (day 5) of DS treatment. It is well known that activated DCs have a fundamental role in coordinating the innate and adaptive immune response by capturing antigen within the peripheral tissues and migrating to the regional lymph nodes via afferent lymphatic vessels where they present antigens to naive T cells in the context of the necessary costimulatory molecules. This evidence suggests that $CD8^+$ cell depletion promoted generation of $CD4^+$ T cells via activation of DCs. To investigate the definitive role of intraepithelial $CD8^+$ cells in activation of DCs, we also performed subconjunctival injection of anti-CD8 in this study; however, to our surprise, subconjunctivally injected anti-CD8 antibody almost completely depleted the $CD8^+$ cells in the draining CLN, similar to systemic CD8 antibody-depleted group. This suggests that subconjunctivally injected anti-CD8 antibody gained access to the draining CLN where it effectively depleted $CD8^+$ Tregs and promoted generation of $CD4^+$ effector T cells.

In this study, we found the $CD8^+$ cell population contains regulatory cells that have a pivotal role in suppressing generation of pathogenic Th17 cells in our DS model. This is a major finding because mechanisms that control $CD4^+$ T-cell-mediated tissue damage are a significant factor in averting and resolving chronic inflammatory diseases. Several lines of evidence support the claim that $CD8^+$ Tregs dampen the SS-like disease in our model: (1) $CD8^+$ cell depletion during DS promoted generation of pathogenic $CD4^+$ T cells with increased IL-17A expression in both the ocular surface and draining CLN of donor mice; (2) adoptive transfer of $CD4^+$ T cells from $CD8^+$ cell-depleted DS-treated donors increased ocular surface infiltration with $CD4^+$ T cells that manifested increased IL-17A and CCL20 production; (3) abundant $CD4^+$ T cells infiltrated the corneal epithelia and central stroma in both the donor and recipient mice in the $CD8^+$ cell-depleted group in our current study. These pathogenic $CD4^+$ T cells appear to have a Th17 phenotype. It has been demonstrated that Th17 differed from Th1 by exhibiting a stronger affinity for the cornea of inflamed eyes, and after adoptive transfer, Th17 polarized CD4 cells were found to abundantly invade the corneal stroma and epithelia in the recipient eyes, whereas Th1 polarized CD4 cells not;[8] and (4) enhanced pathogenicity of $CD4^+$ T cells derived from $CD8^+$ cell-depleted mice was associated with increased levels of IL-17A in both donor and recipient mice. IL-17A has been shown to stimulate production of IL-1, tumor necrosis factor alpha, IL-6, IL-8 and MMPs by epithelial cells and fibroblasts.[30–32] We have previously shown that IL-17A contributes to the development of epithelial corneal in our DS model[13] via increased MMP-9 production and activation. MMP-9 has been found to have a central role in DS-induced corneal barrier disruption, as MMP-9-deficient mice were resistant to barrier disruption in DS.[33,34] We have also reported that IL-17 neutralization during DS decreased the expression of MMP-9 and MMP-3 and improved corneal barrier function.[13] In our current study, we found that increased IL-17A production in donor $CD4^+$ T cells resulted in greater corneal barrier disruption and increased MMP-3 and MMP-9 expression in the recipient corneal epithelia, further supporting the link between $CD8^+$ Treg suppression of pathogenic Th17 cells in this SS model.

Multiple $CD8^+$ Treg subtypes are now recognized as essential regulators of the immune system that prevent autoimmunity through secretion of multiple cytokines and subsequent inhibition of effector lymphocyte function.[4–7] According to their origin, $CD8^+$ Treg subsets have been grouped into natural and inducible Tregs. Natural Tregs are generated and mature within the thymus and are characterized

by the expression of either human leukocyte antigen-G or CD122 and CD28.[35] The mechanism of suppression is cell contact independent and mediated by soluble factors, such as soluble human leukocyte antigen-G or IL-10.[35] In contrast to naturally occurring Tregs, inducible Tregs are generated from naive cells in the periphery after encounter with antigens, presented by DCs that have an activation status distinct from those DCs that promote Th cell differentiation.[36] The mechanism of suppression of T effector cells by inducible Tregs is by cell–cell contact and/or release of soluble factors.[36] $CD8^+CD122^+$ T cells are a recently identified natural Treg that appear to have a function in immune homeostasis, because activated T cells expand without restraint and cause lethal disorders in mice in their absence.[19] In our current study, rare $CD8^+CD122^+$ T cells were noted in CLN and ocular surface, and no obvious change was found in the number of $CD8^+CD122^+$ Tregs in CLN after DS, suggesting that $CD8^+CD122^+$ Treg may not contribute to the regulation of autoimmune inflammation in this model.

Thus far, the effects of $CD8^+CD103^+$ Treg on suppressing autoimmune Th17 biased disease have not been established. In our study, $CD8^+CD103^+$ Tregs were noted in the mouse ocular surface, and i.p. injected $CD8^+CD103^+$ Treg homed to the conjunctiva. More than 60% of $CD8^+$ lymphocytes in the CLN were found to co-express CD103, and the number of these $CD8^+CD103^+$ Tregs significantly increased after DS. Co-adoptive transfer of $CD8^+CD103^+$ Tregs failed to prevent accumulation of adoptively transfer $CD4^+$ T cells infiltrating the ocular surface suggesting that $CD8^+$ T cells regulates generation of pathogenic $CD4^+$ T cells in the afferent arm but not migration of cells to the ocular surface. CD103 is the integrin α_E that forms the heterodimer $\alpha_E\beta_7$ molecule with β_7 integrin and it has been identified as a marker for intraepithelial lymphocytes in a number of mucosal sites.[28] Recently, $CD8^+CD103^+$ T cells have also been reported to exert regulatory activity on $CD4^+$ T-cell proliferation in a cell–cell contact-dependent manner.[21–23,35] That alloreactive $CD8^+CD103^+$ Tregs are inducible and generated at the effector site of an immune response was suggested by data indicating that $CD8^+$ T cells responding to donor alloantigens presented by DCs within draining lymph nodes rapidly upregulated CD103 expression, and subsequently migrated into the transplanted graft.[37] The findings of this study suggest that the activated DCs in ocular surface in response to DS migrate to CLN and consequently promote generation of $CD8^+CD103^+$ Treg. To develop novel immunomodulatory therapies for SS, it may be valuable to further investigate the mechanisms by which $CD8^+CD103^+$ Treg suppress generation of Th17 effector cells in response to DS in this murine SS model.

In summary, the $CD8^+$ cell population contains regulatory cell subsets that suppress generation of the pathogenic Th17 response that has a pivotal role in DS-induced disruption of mucosal barrier function. This study provides new insight into the pathogenesis of Th17 biased autoimmune diseases.

METHODS

Mice. This research protocol was approved by the Baylor College of Medicine Center for Comparative Medicine, and it conformed to the standards in the Association for Research in Vision and Ophthalmology Statement for the Use of Animals in Ophthalmic and Vision Research.

Female C57BL/6 (C57BL/6NTac, B6) and B6.Cg/NTac-Foxn1^{nu} NE9 (nude) were purchased from Taconic (Germantown, NY). Mice were used at 6 to 10 weeks of age.

Murine DS model. DS was created in B6 mice by subcutaneous injection of scopolamine hydrobromide (0.5 mg/0.2 ml; Sigma-Aldrich, St Louis, MO), q.i.d. (0800, 1200, 1400, and 1700 hours) and exposure to an air draft and $<35\%$ ambient humidity for 1, 5, or 10 consecutive days (DS1, DS5, and DS10, respectively).[12–14] A group of female mice that did not receive any treatment to induce dry eye served as a NS controls.

Antibody depletion of $CD8^+$ cells in B6 mice. Eight groups of B6 mice were evaluated: DS1/DS5 mice that received systemic (i.p.; S) injections of anti-CD8α antibody (500 μg per dose, 1 mg/ml, clone YTS 169.4; DS1 + S-αCD8 and DS5 + S-αCD8, respectively) or rat-IgG isotype control (500 μg per dose, 1 mg/ml, Sigma-Aldrich; DS1 + S-IC and DS5 + S-IC, respectively); and DS1/DS5 mice that received topical (subconjunctival; T) injections of anti-CD8 antibody (50 μg per dose, 2.5 mg/ml, clone YTS 169.4; DS1 + T-αCD8 and DS5 + T-αCD8, respectively) or rat-IgG isotype control (50 μg per dose, 2.5 mg/ml, Sigma-Aldrich; DS1 + T-IC and DS5 + T-IC, respectively). Mice received a total of three injections at days –4, –2, and 0 when subjected to DS for 1 day and a total of four injections at days –4, –2, 0, and + 2 when subjected to DS for 5 days.

Isolation of murine $CD4^+$ T cells and adoptive transfer. Superior CLN and spleens from donor mice were collected and meshed gently between two frosted end glass slides, as previously described.[14] Untouched $CD4^+$ cells were isolated using magnetic beads according to the manufacturer's instructions (MACS system; Miltenyi Biotec, Bergisch Gladbach, Germany). The cells were analyzed by flow cytometry and were found to be $>90\%$ pure (data not shown). One donor-equivalent of cells were transferred i.p. to T-cell-deficient nude mice (approximately 5×10^6 $CD4^+$ T cells). The adoptive transfer recipients were killed after 72 h. In some experiments, eyes were collected for histology, were evaluated for corneal permeability while in others cornea and conjunctiva were processed for RNA analysis. Nude mouse recipients were divided into four groups: (1) NS that received $CD4^+$ T cells from NS B6 mice; (2) DS5 that received $CD4^+$ T cells from DS5 B6 mice; (3) DS5 + αCD8 that received $CD4^+$ T cells from DS5 + S- αCD8 B6 mice and (4) DS5 + IC that received $CD4^+$ T cells from DS5 + S-IC B6 mice.

Isolation and reconstitution of murine $CD8^+CD103^+$ Treg. To investigate the role of $CD8^+CD103^+$ Treg in generation of pathogenic $CD4^+$ T cells during DS, $CD8^+CD103^+$ Treg were simultaneously co-adoptively transferred with $CD4^+$ T cells isolated from B6 mice subjected to DS10.

$CD8^+$ T cells were isolated from splenocytes and superficial CLN using anti-CD8 antibody-conjugated magnetic microbeads and columns according to the manufacturer's protocol (MACS system). $CD8^+$ cells were then incubated with anti-CD103-antigen-presenting cell (APC) antibody (clone 2E7, Biolegend, San Diego, CA) followed by an incubation with APC-conjugated beads (MACS system). Flow cytometry was used to confirm CD8 isolation and effective separation of cells into $CD8^+CD103^+$ and $CD8^+CD103^-$ populations (**Figure 5**).

Nude mouse recipients were divided into four groups in this experiment: (1) NS that received $CD4^+$ T cells from NS B6 mice; (2) DS10 that received $CD4^+$ T cells from DS10 B6 mice; (3) DS10 + $CD8^+CD103^+$ Treg mice that received $CD4^+$ T cells from DS10 B6

mice and $CD8^+CD103^+$ (2×10^6); (4) DS10 + $CD8^+CD103^-$ mice that received $CD4^+$ T cells from DS10 B6 mice and $CD8^+CD103^-$ (2×10^6). $CD4^+$ T cells were isolated as above described, and 2×10^6 cells suspended in 100 µl of sterile phosphate-buffered saline were injected (i.p.) into nude recipient mice. Eyes were collected for histology 72 h after the adoptive transfer ($n = 5$ samples).

Histology and immunohistochemistry. Eyes and anexae from each group ($n = 5$) were excised, embedded in optimal cutting temperature compound (VWR, Suwanee, GA), and flash frozen in liquid nitrogen. Sagittal 8 µm sections were cut with a cryostat (HM 500; Micron, Waldorf, Germany) and placed on glass slides that were stored at $-80\,^{\circ}C$.

Immunohistochemistry was performed to detect and count the cells in the conjunctiva that stained positively for CD4 (clone H129.9, 10 µg/ml, BD Pharmingen, San Diego, CA) and CD11c (clone HL3CN, 10 µg/ml, BD Pharmingen). Cryosections were stained with the above-mentioned primary antibodies and appropriate biotinylated secondary antibodies (BD Pharmingen; Jackson Immune Laboratories, West Grove, PA) and Vectastain Elite ABC using NovaRed reagents (Vector, Burlingame, CA). Secondary antibody alone and appropriate anti-mouse isotype (BD Pharmingen) controls were also performed. Three sections from each animal were examined and photographed with a microscope equipped with a digital camera (Eclipse E400 with a DS-Fi1; Nikon, Melville, NY). Positively stained cells were counted in the conjunctiva using image analysis software (NIS Elements Software, version 3.0; Nikon) software.

Isolation of murine ocular surface cells. The eyes and lids of mice were excised, pooled, and incubated in 10 ml of 5 mg/ml of Dispase II (Roche Molecular Biochemicals, Indianapolis, IN) as previously described.[24] Collected cells were used either for flow cytometry or ELISPOT.

Flow cytometry analysis of murine cells. Single-cell suspensions of CLN were stained with anti-CD16/32 (BD Pharmingen) at $4\,^{\circ}C$ for 10 min, followed by staining with anti-CD8α-fluorescein isothiocyanate (FITC; clone 53-6.7; BD Pharmingen) or anti-CD4-FITC (GK1.5; BD Pharmingen), anti-CD8α-phycoerythrin (PE; clone 53-6.7; BD Pharmingen), anti-CD122-PE (clone TM-β1; BD Pharmingen), and anti-CD103-APC (clone 2E7; Biolegend), anti-CD11c-FITC (clone HL3; BD Pharmingen), anti-CD11b-APC (clone M1/70; BD Pharmingen) or anti-IAIE-PE (clone 2G9; BD Pharmingen). Single-cell suspensions isolated from cornea and conjunctiva were stained with anti-CD16/32, followed by staining with anti-CD3-pacific blue (clone 500A2; BD Pharmingen), anti-CD8α-PE (clone 53-6.7) and anti-CD103-APC (clone 2E7; Biolegend).

Negative controls consisted of splenocytes stained with isotype antibodies (BD Pharmingen). Cells were resuspended in propidium iodide and kept on ice until flow cytometry analysis was performed. A BD LSRII Benchtop cytometer was used and data analyzed using FlowJo software (TreeStar, Ashland, OR).

Mouse IL-17A, IL-13, and IFN-γ ELISPOT. Replicate 50 µl cell suspensions containing 1.0×10^6 freshly ocular surface cells and $CD4^+$ T cells isolated as described above were added to 96-well polyvinylidene difluoride plates (Millipore, Billerica, MA), pre-coated with anti-mouse IL-17A, IL-13, or IFN-γ capture antibody (R&D Systems; Minneapolis, MN), as previously described.[24] The positive, red spots were counted under a dissecting microscope (SMZ 1500, Melville, NY). Replicate wells were averaged from two individual experiments. Results are presented as number of spots/1×10^6 cells.

Corneal permeability. Corneal epithelial permeability to Oregon-green-dextran (70,000 molecular weight; Invitrogen, Eugene, OR) was assessed in the nude recipient mice ($n = 10$ eyes per 5 mice per group per experiment in three independent experiments) as previously described.[13] Briefly, 0.5 µl of 50 mg/ml Oregon-green-dextran was instilled onto the ocular surface 1 min before killing. Corneas were rinsed with phosphate-buffered saline and photographed with a high dynamic and resolution digital camera (Coolsnap HQ2, Photometrics, Tucson, AZ) attached to a stereoscopic zoom microscope (SMZ 1500; Nikon) under fluorescence excitation at 470 nm. The severity of corneal Oregon-green-dextran staining was graded in digital images by two masked observers, using NIS Elements (version 3.0, Nikon) within a 2-mm diameter circle placed on the central cornea. The mean fluorescent intensity measured by the software inside this central zone was transferred to a database and the results averaged within each group.

RNA isolation and quantitative PCR. Cornea epithelium from B6.nude recipient mice was scrapped with a scalpel, conjunctiva was surgically excised, and $CD4^+$ T cells were isolated as described above. Six to 12 samples were used in each group. Total RNA was extracted using a Pico Pure RNA isolation kit (Arcturus, Applied Biosystems, Foster City, CA) according to the manufacturer's instructions, quantified by a NanoDrop ND-1000 Spectrophotometer (Thermo Scientific, Wilmington, DE) and stored at $-80\,^{\circ}C$. Samples were treated with DNase to eliminate genomic DNA contamination, according to the manufacturer's instructions (Qiagen, Valencia, CA). First-strand complementary DNA was synthesized with random hexamers by M-MuLV reverse transcription (Ready-To-Go You-Prime First-Strand Beads; GE Healthcare, Arlington Heights, NJ), as previously described.[10]

Quantitative real-time PCR was performed with specific MGB probes (Taqman; Applied Biosystems) and PCR master mix (Taqman Gene Expression Master Mix), in a commercial thermocycling system (StepOnePlus Real-Time PCR System, Applied Biosystems), according to the manufacturer's recommendations. Quantitative real-time PCR was performed using gene expression assay primers and MGB probes specific for murine targets IL-17A (Mm00439618), IFN-γ (Mm00801778), IL-13 (Mm99999190), MMP-3 (Mm00440295), MMP-9 (Mm00442991), CCL20 (Mm00444228), GATA-3 (Mm00484683), RORγT (Mm00441139) and T-bet (Mm00450960).

The copy number of the genes of interest was calculated by comparing the samples to the gene-specific standard curves, previously prepared using commercial mouse complementary DNA (Zyagen, San Diego, CA). Samples and standards were assayed in duplicate. A non-template control and total RNA without retrotranscription were included in all the experiments to evaluate PCR and DNA contamination of the reagents.

MMPs immunofluorescent staining and *in situ* zymography. Immunofluorescent staining was performed with polyclonal goat anti-MMP-3 (2 µg/ml; SC6834; Santa Cruz Biotechnology, Santa Cruz, CA) or rabbit anti-MMP-9 (5 µg/ml, Chemicon-Billerica, MA, USA) and with appropriate Alexa-Fluor 488-conjugated IgG secondary antibodies as previously described.[38] *In situ* zymography was performed to localize the gelatinase activity in the corneal epithelia, as previously described.[38]

The images were captured with a fluorescence microscope (Eclipse E400; Nikon) and a attached digital camera (Eclipse E400 with a DS-F1; Nikon). Fluorescent intensity was measured were analyzed using the NIS Elements Software (Nikon).

Statistical analysis. One-way analysis of variance with Tukey's *post hoc* testing was used for statistical comparisons using GraphPad Prism 5.0 software (GraphPad Software Incorporation, San Diego, CA). $P \leq 0.05$ was considered statistically significant.

ACKNOWLEDGEMENTS

This study was supported by the NIH grant EY018888 (CSDP), EY11915 (SCP), EY018090 (SCP, MES,JYN), NIH core grants EY002520 and EY020799, Research to Prevent Blindness, the Oshman Foundation, William Stamps Farish Fund, the Hamill Foundation and by the Cytometry and Cell Sorting Core at Baylor College of Medicine, which was funded by the NIH NIAID P30AI036211, NCI P30CA125123, and NCRR S10RR024574.

DISCLOSURE

CS Schaumburg, KF Siemasko, and ME Stern are employees of Allergan. The remaining authors declared no conflict of interest.

REFERENCES

1. Bettelli, E., Oukka, M. & Kuchroo, V.K. T(H)-17 cells in the circle of immunity and autoimmunity. *Nat. Immunol.* **8**, 345–350 (2007).
2. Jabs, D.A., Lee, B., Whittum-Hudson, J.A. & Prendergast, R.A. Th1 versus Th2 immune responses in autoimmune lacrimal gland disease in MRL/Mp mice. *Invest. Ophthalmol. Vis. Sci.* **41**, 826–831 (2000).
3. O'Garra, A. & Vieira, P. Regulatory T cells and mechanisms of immune system control. *Nat. Med.* **10**, 801–805 (2004).
4. Tang, X.L., Smith, T.R. & Kumar, V. Specific control of immunity by regulatory CD8 T cells. *Cell Mol. Immunol.* **2**, 11–19 (2005).
5. Dinesh, R.K., Skaggs, B.J., La, C.A., Hahn, B.H. & Singh, R.P. CD8+ Tregs in lupus, autoimmunity, and beyond. *Autoimmun. Rev.* **9**, 560–568 (2010).
6. Suzuki, M., Konya, C., Goronzy, J.J. & Weyand, C.M. Inhibitory CD8+ T cells in autoimmune disease. *Hum. Immunol.* **69**, 781–789 (2008).
7. Konya, C., Goronzy, J.J. & Weyand, C.M. Treating autoimmune disease by targeting CD8(+) T suppressor cells. *Expert Opin. Biol. Ther.* **9**, 951–965 (2009).
8. Cox, C.A. *et al.* Both Th1 and Th17 are immunopathogenic but differ in other key biological activities. *J. Immunol.* **180**, 7414–7422 (2008).
9. Dardalhon, V., Korn, T., Kuchroo, V.K. & Anderson, A.C. Role of Th1 and Th17 cells in organ-specific autoimmunity. *J. Autoimmun.* **31**, 252–256 (2008).
10. Luo, L., Li, D.Q., Doshi, A., Farley, W., Corrales, R.M. & Pflugfelder, S.C. Experimental dry eye stimulates production of inflammatory cytokines and MMP-9 and activates MAPK signaling pathways on the ocular surface. *Invest. Ophthalmol. Vis. Sci.* **45**, 4293–4301 (2004).
11. de Paiva, C.S. *et al.* Age-related T-cell cytokine profile parallels corneal disease severity in Sjogren's syndrome-like keratoconjunctivitis sicca in CD25KO mice. *Rheumatology (Oxford)* **49**, 246–258 (2010).
12. de Paiva, C.S. *et al.* Dry eye-induced conjunctival epithelial squamous metaplasia is modulated by interferon-{gamma}. *Invest. Ophthalmol. Vis. Sci.* **48**, 2553–2560 (2007).
13. de Paiva, C.S. *et al.* IL-17 disrupts corneal barrier following desiccating stress. *Mucosal. Immunol.* **2**, 243–253 (2009).
14. Niederkorn, J.Y. *et al.* Desiccating stress induces T cell-mediated Sjogren's syndrome-like lacrimal keratoconjunctivitis. *J. Immunol.* **176**, 3950–3957 (2006).
15. de Paiva, C.S. *et al.* IFN- γ promotes goblet cell loss in response to desiccating ocular stress. *Invest. Ophthalmol. Vis. Sci.* **47**; E-Abstract 5579 (2006).
16. Sacks, E.H., Wieczorek, R., Jakobiec, F.A. & Knowles, D.M. Lymphocytic subpopulations in the normal human conjunctiva. A monoclonal antibody study. *Ophthalmology* **93**, 1276–1283 (1986).
17. Rojas, B. *et al.* Cell populations and adhesion molecules expression in conjunctiva before and after bone marrow transplantation. *Exp. Eye Res.* **81**, 313–325 (2005).
18. Raphael, M., Bellefqih, S., Piette, J.C., Le, H.P., Debre, P. & Chomette, G. Conjunctival biopsy in Sjogren's syndrome: correlations between histological and immunohistochemical features. *Histopathology* **13**, 191–202 (1988).
19. Rifa'i, M., Kawamoto, Y., Nakashima, I. & Suzuki, H. Essential roles of CD8+CD122+ regulatory T cells in the maintenance of T cell homeostasis. *J. Exp. Med.* **200**, 1123–1134 (2004).
20. Endharti, A.T. *et al.* CD8+CD122+ regulatory T cells (Tregs) and CD4$^+$ Tregs cooperatively prevent and cure CD4+ cell-induced colitis. *J. Immunol.* **186**, 41–52 (2011).
21. Lu, L. *et al.* CD8(+)CD103(+) regulatory T cells in spontaneous tolerance of liver allografts. *Int. Immunopharmacol.* **9**, 546–548 (2009).
22. Ho, J., Kurtz, C.C., Naganuma, M., Ernst, P.B., Cominelli, F. & Rivera-Nieves, J.A. CD8+/CD103high T cell subset regulates TNF-mediated chronic murine ileitis. *J. Immunol.* **180**, 2573–2580 (2008).
23. Uss, E., Rowshani, A.T., Hooibrink, B., Lardy, N.M., van Lier, R.A. & ten Berge, I.J. CD103 is a marker for alloantigen-induced regulatory CD8+ T cells. *J. Immunol.* **177**, 2775–2783 (2006).
24. Zhang, X. *et al.* NK cells promote Th-17 mediated corneal barrier disruption in dry eye. *PLoS One* **7**, e36822 (2012).
25. de Paiva, C.S. *et al.* Disruption of TGF-beta signaling improves ocular surface epithelial disease in experimental autoimmune keratoconjunctivitis sicca. *PLoS One* **6**, e29017 (2011).
26. Homey, B. *et al.* Up-regulation of macrophage inflammatory protein-3 alpha/CCL20 and CC chemokine receptor 6 in psoriasis. *J. Immunol.* **164**, 6621–6632 (2000).
27. Liang, S.C. *et al.* Interleukin (IL)-22 and IL-17 are coexpressed by Th17 cells and cooperatively enhance expression of antimicrobial peptides. *J. Exp. Med.* **203**, 2271–2279 (2006).
28. Schon, M.P. *et al.* Mucosal T lymphocyte numbers are selectively reduced in integrin alpha E (CD103)-deficient mice. *J. Immunol.* **162**, 6641–6649 (1999).
29. Subramanian, S. *et al.* Sustained expression of circulating human alpha-1 antitrypsin reduces inflammation, increases CD4+FoxP3+ Treg cell population and prevents signs of experimental autoimmune encephalomyelitis in mice. *Metab. Brain Dis.* **26**, 107–113 (2011).
30. Cortez, D.M. *et al.* IL-17 stimulates MMP-1 expression in primary human cardiac fibroblasts via p38. *Am. J. Physiol. Heart Circ. Physiol.* **293**, H3356–H3365 (2007).
31. Yagi, Y., Andoh, A., Inatomi, O., Tsujikawa, T. & Fujiyama, Y. Inflammatory responses induced by interleukin-17 family members in human colonic subepithelial myofibroblasts. *J. Gastroenterol.* **42**, 746–753 (2007).
32. Jones, C.E. & Chan, K. Interleukin-17 stimulates the expression of interleukin-8, growth-related oncogene-alpha, and granulocyte-colony-stimulating factor by human airway epithelial cells. *Am. J. Respir. Cell Mol. Biol.* **26**, 748–753 (2002).
33. Pflugfelder, S.C. *et al.* Matrix metalloproteinase-9 knockout confers resistance to corneal epithelial barrier disruption in experimental dry eye. *Am. J. Pathol.* **166**, 61–71 (2005).
34. de Paiva, C.S. *et al.* Corticosteroid and doxycycline suppress MMP-9 and inflammatory cytokine expression, MAPK activation in the corneal epithelium in experimental dry eye. *Exp. Eye Res.* **83**, 526–535 (2006).
35. Koch, S.D., Uss, E., van Lier, R.A. & ten Berge, I.J. Alloantigen-induced regulatory CD8+CD103+ T cells. *Hum. Immunol.* **69**, 737–744 (2008).
36. Mills, K.H. Regulatory T cells: friend or foe in immunity to infection? *Nat. Rev. Immunol.* **4**, 841–855 (2004).
37. Wang, D. *et al.* Regulation of CD103 expression by CD8+ T cells responding to renal allografts. *J. Immunol.* **172**, 214–221 (2004).
38. Corrales, R.M., Stern, M.E., de Paiva, C.S., Welch, J., Li, D.Q. & Pflugfelder, S.C. Desiccating stress stimulates expression of matrix metalloproteinases by the corneal epithelium. *Invest. Ophthalmol. Vis. Sci.* **47**, 3293–3302 (2006).